

Kinematic Calibration of a Cartesian Parallel Manipulator

Han Sung Kim

Abstract: In this paper, a prototype Cartesian Parallel Manipulator (CPM) is demonstrated, in which a moving platform is connected to a fixed frame by three *PRRR* limbs. Due to the orthogonal arrangement of the three prismatic joints, it behaves like a conventional X-Y-Z Cartesian robot. However, because all the linear actuators are mounted at the fixed frame, the manipulator may be suitable for applications requiring high speed and accuracy. Using a geometric method and the practical assumption that three revolute joint axes in each limb are parallel to one another, a simple forward kinematics for an actual model is derived, which is expressed in terms of a set of linear equations. Based on the error model, two calibration methods using full position and length measurements are developed. It is shown that for a full position measurement, the solution for the calibration can be obtained analytically. However, since a ball-bar is less expensive and sufficiently accurate for calibration, the kinematic calibration experiment on the prototype machine is performed by using a ball-bar. The effectiveness of the kinematic calibration method with a ball-bar is verified through the well-known circular test.

Keywords: Ball-bar, cartesian robot, error model, kinematic calibration, parallel manipulator.

1. INTRODUCTION

Parallel manipulators have been studied extensively for applications that require high speed, accuracy, and stiffness. Among various types of parallel manipulators, the Gough-Stewart platform has attracted the most attention because it has six degrees of freedom (DOF) and all the linear actuators are under pure forces. However, the manipulator does have some disadvantages, such as complex forward kinematics, small workspace, and complicated universal and spherical joints.

To overcome these shortcomings, parallel manipulators with fewer than six DOF have been investigated. For example, a 3-DOF parallel manipulator with 3-*RPS* (revolute-prismatic-spherical) chains was analyzed and developed in [1,2]. Many other novel 3-DOF parallel manipulators have also been developed. For example, the DELTA robot is a simple and fast 3-DOF parallel manipulator [3]. However, most of these manipulators have coupled motion between the position and orientation of the end-effector. Recent research on 3-DOF parallel

manipulators has been leaning toward the decoupling of the position and orientation of the end-effector and the elimination of complicated multi-DOF joints. Since the positioning task is essential in many areas, several 3-DOF translational parallel manipulators (TPMs) have been developed. For example, Tsai et al. [4,5] designed a 3-DOF TPM that employs only revolute joints and planar parallelograms. Tsai [6] presented the 3-DOF TPM using 3-*UPU* (universal-prismatic-universal) serial chains. Zhao and Huang [7] studied the kinematics of an over-constrained 3-*RRC* (revolute-revolute-cylindrical) translational manipulator. Kim and Tsai [8,9] conceived a 3-*PRRR* (prismatic-revolute-revolute-revolute) parallel manipulator, which employs only revolute and prismatic joints to achieve pure translational motion of the moving platform and behaves like a traditional X-Y-Z Cartesian machine. Wenger and Chablat [10] suggested the use of a 3-DOF TPM as a machine tool, called the Orthoglide. However, the majority of works on TPMs have focused on the kinematic and design problems.

Various kinematic calibration methods for parallel manipulators have been reported and good summary on the previous works can be found in [11]. Most of the works deal with the problems of kinematic calibration of 6-DOF parallel manipulators. However, the accuracy improvement of a 3-DOF TPM by the development of an error model and the kinematic calibration has been little investigated. Iurascu and Park [12] classify the kinematic calibration methods into three categories; task space calibration, joint

Manuscript received November 25, 2004; revised April 6, 2005; accepted June 20, 2005. Recommended by Editorial Board member Wankyun Chung under the direction of Editor Keum-Shik Hong. This work was supported by the Kyungnam University Research Fund, 2005.

Han Sung Kim is with the School of Mechanical and Automation Engineering, Kyungnam University, 449 Wolyung-dong, Masan, Kyungnam 631-701, Korea (e-mail: hkim@kyungnam.ac.kr).

space calibration, and combined task-joint space calibration. Since among the measurement methods, a ball-bar is less expensive and sufficiently accurate for precise calibration, it is used for the kinematic calibration of 6-DOF parallel manipulators [13-15]. However, it requires task space calibration, i.e., the use of numerical forward kinematics calculation, which may cause some problems in the optimization iterative scheme. In this work, the forward kinematics for an actual model is obtained as a set of linear equations, based on the practical assumption and geometrical approach.

In this paper, a prototype CPM is demonstrated. Due to the orthogonal arrangement of the three linear actuators, there exists a one-to-one correspondence between the input and output displacements, velocities, and forces and the Jacobian matrix is always isotropic over the entire workspace. Under the assumption that three revolute joint axes in each limb are parallel to one another, a simple forward kinematics for an actual model is derived, which is expressed in terms of a set of linear equations. It is shown that when a full position measurement is used, the kinematic calibration can be solved analytically. For a length measurement, i.e., using a ball-bar [13-15], the kinematic calibration is reduced to a nonlinear least squares method minimizing the calculated and measured lengths of a ball-bar. It is shown that by properly choosing a base coordinate system, the number of kinematic parameters can be reduced from twelve to six. Finally, using the QC10 ball-bar, the calibration experiment on the prototype CPM is performed. In order to show the effectiveness of the developed calibration method using a ball-bar, the results of the well-known circular tests before and after calibration are presented.

2. KINEMATICS OF A NOMINAL MODEL

The kinematic structure of a CPM is shown in Fig. 1 where a moving platform is connected to a fixed base by three *PRRR* limbs. The moving platform is symbolically represented by a circle defined by B_1 , B_2 , and B_3 and the fixed base is defined by three guide rods passing through A_1 , A_2 , and A_3 , respectively. The three revolute joint axes in each limb are located at points A_i , M_i , and B_i , respectively, and are parallel to the ground-connected prismatic joint axis. Furthermore, the three prismatic joint axes, passing through point A_i for $i=1, 2, \text{ and } 3$, are parallel to the X , Y , and Z axes, respectively. Specifically, the first prismatic joint axis lies on the X axis; the second prismatic joint axis is parallel to the Y axis with an offset e_z in the Z direction; and the third prismatic joint axis is parallel to the Z axis with

an offset e_x in the X direction and e_y in the Y direction. Point P represents the center of the moving platform. The link lengths are denoted by l_{i1} , l_{i2} , and l_{i3} , respectively. The offset of a prismatic joint is defined by d_{0i} and the sliding distance from the offset is defined by d_i . Note that each *PRRR* limb is equivalent to a *CRR* limb. In this regard, the 3-*PRRR* parallel manipulator is a kinematic inversion of the 3-*RRC* manipulator. Note that the third prismatic joint axis is purposely located far away from the Z axis to avoid interference among the three limbs.

Due to the three parallel revolute joints located at points A_i , M_i , and B_i , the X , Y , and Z limbs constrain the moving platform from rotating about the Y and Z , Z and X , and X and Y axes, respectively. Since each limb provides two rotational constraints to the moving platform, the combined effects result in three redundant constraints on the rotation of the moving platform and, therefore, completely constrain the moving platform from rotation. This leaves the moving platform with three translational degrees of freedom.

The forward and inverse kinematic analyses are trivial since there is a one-to-one correspondence between the end-effector position and the input joint displacements. Referring to Fig. 1, each limb constrains point P to lie on a plane that passes through point A_i and is perpendicular to the axis of the linear actuator.

Consequently, the location of P is determined by the intersection of the three planes. A simple kinematic relation can be written as

$$\begin{bmatrix} p_x \\ p_y \\ p_z \end{bmatrix} = \begin{bmatrix} d_1 + d_{01} \\ d_2 + d_{02} \\ d_3 + d_{03} \end{bmatrix}. \quad (1)$$

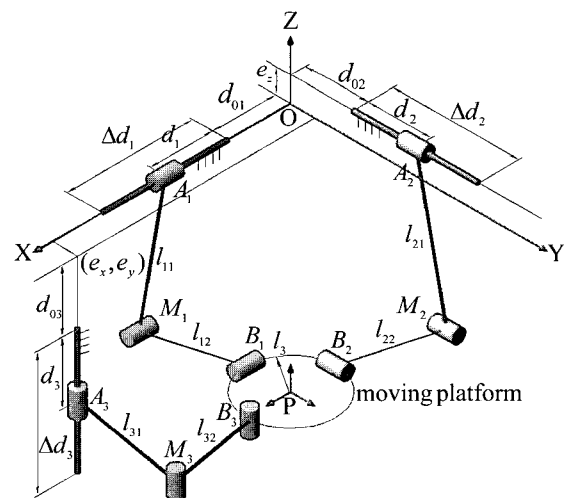


Fig. 1. Geometry of a CPM.

Table 1. Optimized design parameters.

Design Variables	Optimum Values [mm]
$d_{01} = d_{02}$	225.0
d_{03}	226.8
e_x	914.4
e_y	223.9
e_z	0.0
$l_{11} = l_{21}$	400.0
$l_{12} = l_{22}$	373.0
l_{31}	406.0
l_{32}	384.0
l_3	105.0

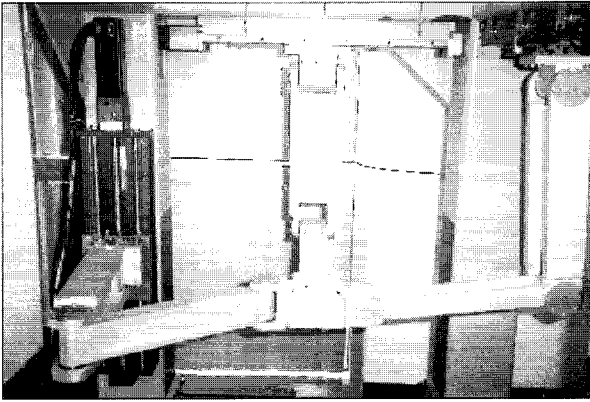


Fig. 2. Prototype CPM.

From the design optimization method to maximize the stiffness of the manipulator for a given box-shape workspace, the optimized design parameters are obtained in Table 1 [8]. The workspace volume is equal to the product of the stroke lengths of linear actuators given by

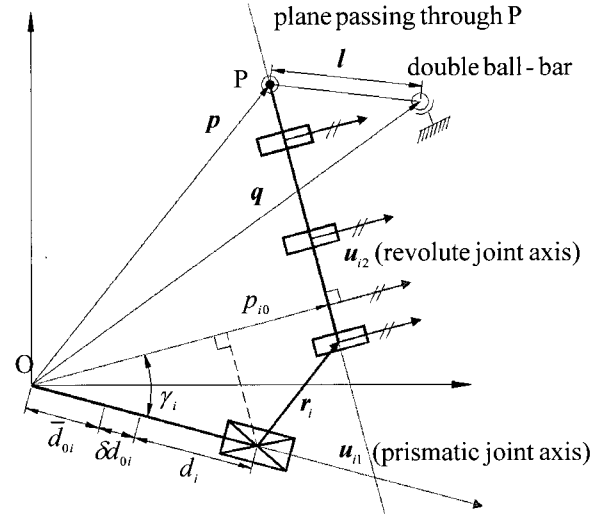
$$\Delta d_1 = \Delta d_2 = 400, \text{ and } \Delta d_3 = 300 [\text{mm}].$$

Fig. 2 shows a prototype CPM designed with the optimized design parameters.

3. KINEMATIC ERROR MODEL

In deriving the kinematic error model, the important assumption that *three revolute joint axes in each limb are parallel to one another* is employed. Otherwise, the third links of the three limbs may have different orientations to one another. So, the manipulator may not move at all or cannot work well due to internal torques if compliance and backlash in joints and links are very small.

Let us consider one simple case when there exist no errors in the Y and Z limbs but the three revolute joint axes in the X limb are a little twisted, which means that the *RRR* serial chain becomes a spatial one. If the

Fig. 3. Kinematic error model of the i^{th} limb.

linear actuators of the Y and Z limbs are locked, five parameters at the end-effector except P_x are fixed. In general, the five fixed parameters at the end-effector cannot be satisfied with only the three joint angles of the *RRR* spatial serial chain in the X limb. However, in the case of the *RRR* planar serial chain, the three end-effector parameters (two positions and one angle) can always be satisfied with three joint angles. In short, when a serial chain with three revolute joints becomes a spatial one, the forward kinematics solution does not always exist. Furthermore, this assumption is practical, since machining two holes in a link almost perfectly parallel to each other is not so difficult. Even if a twist angle is present between two adjacent revolute joint axes, it may be smaller than the incident angles between a prismatic joint axis and the corresponding axis of the base frame and between the axes of the prismatic and revolute joints. This assumption makes the forward kinematic analysis for an actual model and the kinematic calibration much simpler. With this regard, this work will focus on reducing the position error due to the other main error sources.

The unit direction vector of a revolute joint axis is defined as u_{i2} , for $i = 1, 2, \text{ and } 3$, as shown in Fig. 3. For each limb, a plane passing through the end-effector, P , can be defined, whose normal vector is the direction of a revolute joint, u_{i2} . In practice, it may be difficult to fabricate and assemble a perfect orthogonal frame. It is assumed that the X, Y, and Z prismatic joint axes are slightly misaligned with the X, Y, and Z axes, respectively, whose unit direction vectors are defined as u_{i1} , for $i = 1, 2, \text{ and } 3$.

Furthermore, there may exist an offset error, $\delta d_{0i} = d_{0i} - \bar{d}_{0i}$, where d_{0i} and \bar{d}_{0i} denote the actual and nominal values of an offset, respectively. r_i

is defined as the vector from an actual linear actuator position, $(d_i + \bar{d}_{0i} + \delta d_{0i})\mathbf{u}_{i1}$, to the intersection point of the first revolute joint axis and the plane.

For a given actuator length, the shortest distance from the origin to the plane is obtained by

$$p_{i0} = (d_i + \bar{d}_{0i}) \cos \gamma_i + n_i, \quad (2)$$

where γ_i is the incident angle between \mathbf{u}_{i1} and \mathbf{u}_{i2} , and n_i is the total offset error projected onto the \mathbf{u}_{i2} given by

$$n_i = \delta d_{0i} \cos \gamma_i + \mathbf{r}_i^T \mathbf{u}_{i2}. \quad (3)$$

It is noted that the offset error, δd_{0i} , and the vector, \mathbf{r}_i cannot be determined, respectively, from the following calibration, because these are projected onto the revolute joint axis.

For each limb, a plane passing through the end-effector, P , with the normal vector, \mathbf{u}_{i2} , and the shortest distance, p_{i0} , can be given by

$$\mathbf{u}_{i2}^T \mathbf{p} = p_{i0}, \quad (4)$$

where $\mathbf{p} = [p_x, p_y, p_z]^T$. Writing (4) three times each for $i=1, 2, \text{ and } 3$, the end-effector position is determined by the intersection point of the three planes, which yields the forward kinematics for an actual model given by

$$\begin{bmatrix} \mathbf{u}_{12}^T \\ \mathbf{u}_{22}^T \\ \mathbf{u}_{32}^T \end{bmatrix} \begin{bmatrix} p_x \\ p_y \\ p_z \end{bmatrix} = \begin{bmatrix} (d_1 + \bar{d}_{01}) \cos \gamma_1 + n_1 \\ (d_2 + \bar{d}_{02}) \cos \gamma_2 + n_2 \\ (d_3 + \bar{d}_{03}) \cos \gamma_3 + n_3 \end{bmatrix}. \quad (5)$$

It should be noted that the link lengths in each limb have no effect on position accuracy and that the direction of a prismatic joint with respect to the base coordinate system is unimportant whereas the incident angle, r_i , is significant for determining the end-effector position. In short, the normal vector, \mathbf{u}_{i2} , and the shortest distance, p_{i0} to the plane are essential to establishing the end-effector position.

Therefore, the total kinematic parameters to be determined become

$$\boldsymbol{\beta} = [\gamma_1, n_1, \mathbf{u}_{12}^T, \gamma_2, n_2, \mathbf{u}_{22}^T, \gamma_3, n_3, \mathbf{u}_{32}^T]^T. \quad (6)$$

For a given end-effector position, the linear actuator length can be obtained by

$$d_i = \frac{\mathbf{u}_{i2}^T \mathbf{p} - n_i}{\cos \gamma_i} - \bar{d}_{0i}. \quad (7)$$

4. KINEAMTIC CALIBRATION METHOD

In this work, the calibration method is developed for full position and length measurements. In the full position measurement, the end-effector position is fully measured by a 3 dimensional position measurement device, such as an XYZ laser tracking system or a ball-bar system using the trilateration method [11]. On the other hand, a single ball-bar can be used in the kinematic calibration of a robotic manipulator as a length measurement [13-15]. In the following derivation, the superscripts, "c" and "m" are used to denote the calculated and measured values, respectively, and the first and second subscripts, "i" and "j" are employed to indicate the limb and measurement numbers. As illustrated in Fig. 4, the calibration methods using full position and length measurements are used to find the set of kinematic parameters satisfying the following equations, respectively:

$$\mathbf{p}^c(d_j^m + \bar{d}_0, \boldsymbol{\beta}) = \mathbf{p}_j^m, \quad (8)$$

$$\|\mathbf{p}^c(d_j^m + \bar{d}_0, \boldsymbol{\beta}) - \mathbf{q}\| = l_j^m, \quad (9)$$

where $\mathbf{p}(\cdot)$ denotes the forward kinematics function, $\mathbf{d}_j^m = [d_{1,j}^m, d_{2,j}^m, d_{3,j}^m]^T$, $\bar{\mathbf{d}}_0 = [\bar{d}_{01}, \bar{d}_{02}, \bar{d}_{03}]^T$ and $\|\cdot\|$ denotes the Euclidean norm.

4.1. Analytical solution for a full position measurement

If an accurate position measurement device is provided, and there is also no measurement error in reading linear actuator positions, the kinematic calibration problem for the manipulator can be solved analytically. Multiplying both sides of (8) by \mathbf{u}_{i2}^T yields the uncoupled equation per limb,

$$\mathbf{u}_{i2}^T \mathbf{p}_j^m = (d_{i,j}^m + \bar{d}_{0i}) \cos \gamma_i + n_i. \quad (10)$$

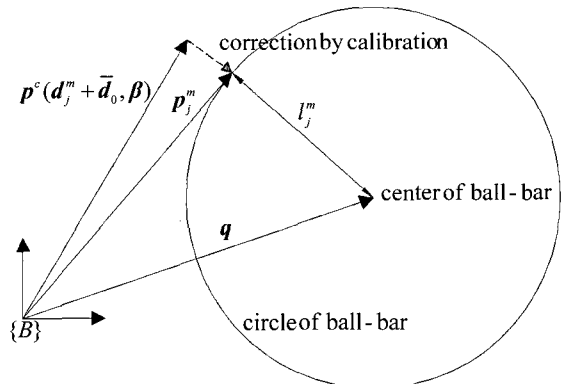


Fig. 4. Outline of the calibration methods using full position and length measurements.

In order to eliminate the kinematic parameter, n_i , one subtracts (10) for $j=j$ from (10) for $j=n$. This results in

$$\mathbf{u}_{i2}^T \mathbf{p}_{nj}^m = d_{i,nj}^m \cos \gamma_i, \quad (11)$$

where $\mathbf{p}_{nj}^m = \mathbf{p}_n^m - \mathbf{p}_j^m = [p_{nj,x}^m, p_{nj,y}^m, p_{nj,z}^m]^T$ and $d_{i,nj}^m = d_{i,n}^m - d_{i,j}^m$. Since $\mathbf{u}_{i2} = [u_{i2,x}, u_{i2,y}, u_{i2,z}]^T$ is a unit directional vector, one variable in \mathbf{u}_{i2} can be reduced by dividing both sides of (10) by one of $u_{i2,x}$, $u_{i2,y}$, and $u_{i2,z}$. For example, dividing (11) by $u_{i2,z}$ yields

$$[p_{nj,x}^m, p_{nj,y}^m, -d_{i,nj}^m] \begin{bmatrix} u_{i2,x}/u_{i2,z} \\ u_{i2,y}/u_{i2,z} \\ \cos \gamma_i / u_{i2,z} \end{bmatrix} = -p_{nj,z}^m. \quad (12)$$

Writing (12) for $j=1,2,3$ gives the following linear simultaneous equations:

$$\begin{bmatrix} p_{n1,x}^m & p_{n1,y}^m & -d_{i,n1}^m \\ p_{n2,x}^m & p_{n2,y}^m & -d_{i,n2}^m \\ p_{n3,x}^m & p_{n3,y}^m & -d_{i,n3}^m \end{bmatrix} \begin{bmatrix} u_{i2,x}/u_{i2,z} \\ u_{i2,y}/u_{i2,z} \\ \cos \gamma_i / u_{i2,z} \end{bmatrix} = \begin{bmatrix} -p_{n1,z}^m \\ -p_{n2,z}^m \\ -p_{n3,z}^m \end{bmatrix}. \quad (13)$$

If the 3×3 matrix depending on the set of measured positions is not singular, the kinematic parameters can be obtained analytically. Once \mathbf{u}_{i2} and r_i are solved

from (13), the kinematic parameter, n_i , can be obtained from (10) for $j=n$. It can be seen that the minimum required number of measured positions is four.

4.2. Solution for a length measurement

When a ball-bar is used as a measurement device, the origin of the world coordinate system can be defined, for example, at the center of a ball fixed at the frame. However, the orientation of the world coordinate system cannot be defined only from the length information of a ball-bar. Hence, in the length measurement such as using a ball-bar, the orientation of a base coordinate system may be arbitrarily selectable. By properly choosing a base coordinate system, the number of kinematic parameters required to express the end-effector position can be reduced.

The new base coordinate system $O'\{X', Y', Z'\}$ expressed in Fig. 5 is defined as follows. The first revolute joint axis of the X limb is parallel to the X' axis, and the Z' axis is determined as the normal vector of the plane made by the revolute joint axes of the X and Y limbs, which can eliminate two parameters in \mathbf{u}_{12} and one in \mathbf{u}_{22} . Specifically, $\mathbf{u}_{12} = [1, 0, 0]^T$, and $\mathbf{u}_{22} = [-\sin \theta_z, \cos \theta_z, 0]^T$. The Y' axis is determined by the right-hand rule, and the Z limb's axis is defined as $\mathbf{u}_{32} = [\cos \theta_x \sin \theta_y, -\sin \theta_x, \cos \theta_x \cos \theta_y]^T$, where θ_x , θ_y , and θ_z are the rotational angles about the fixed X' , Y' , and Z'

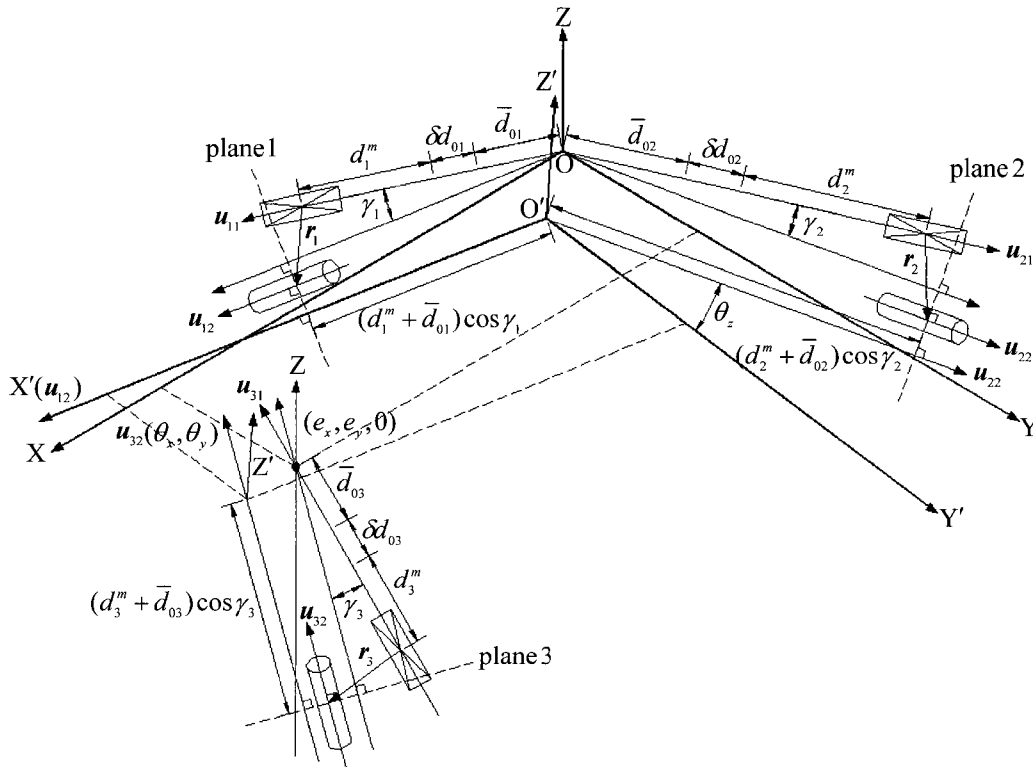


Fig. 5. Definition of a new base coordinate system for a length measurement.

axes. Furthermore, the origin of the base coordinate system is determined by the intersection point of the three new planes, which have the same normal vectors, u_{i2} , and the distances, $(d_i^m + \bar{d}_{0i}) \cos \gamma_i$, with the previously defined three planes passing through P . From the definition, the total offset error, n_i , can be eliminated. The resulting kinematic parameters of the manipulator become six as

$$\beta' = [\gamma_1, \gamma_2, \theta_z, \gamma_3, \theta_x, \theta_y]^T. \quad (14)$$

Generally, the errors associated with the ball-bar are the position error of the ball center fixed at the frame, δq , and the length offset, δl . It is noted that the total offset errors are included in δq . With these errors, (9) can be rewritten as

$$\|p^c(d_j^m + \bar{d}_0, \beta') - (\bar{q} + \delta q)\| = (l_j^m + \delta l), \quad (15)$$

where \bar{q} is the nominal position vector of the ball center with respect to the base coordinate system. It is noted that the position error of the other ball center attached at the moving platform is not considered, since the point is chosen as the end-effector, P .

If the vector h is defined as

$$h(\eta) = \begin{bmatrix} \|p^c(d_1^m + \bar{d}_0, \beta') - (\bar{q} + \delta q)\| - (l_1^m + \delta l) \\ \|p^c(d_2^m + \bar{d}_0, \beta') - (\bar{q} + \delta q)\| - (l_2^m + \delta l) \\ \vdots \\ \|p^c(d_n^m + \bar{d}_0, \beta') - (\bar{q} + \delta q)\| - (l_n^m + \delta l) \end{bmatrix}, \quad (16)$$

the kinematic calibration using a ball-bar can be reduced to a nonlinear least squares minimization problem given by

$$\min_{\eta} h(\eta)^T h(\eta), \quad (17)$$

where $\eta = [\beta'^T, \delta q^T, \delta l]^T$. For solving (17), the "lsqnonlin" function in the Matlab optimization toolbox is used.

5. CALIBRATION EXPERIMENT

The calibration experiment on the prototype machine using a ball-bar has been performed. In this experiment, the QC10 ball-bar of Renishaw having an accuracy of $\pm 0.5[\mu\text{m}]$ is used, as shown in Fig. 6. For the collection of measurement data, one center of the ball-bar is fixed at $\bar{q} = [430, 430, -530]^T$ [mm] expressed in the base coordinate system. The $n = 32$ measurement points are selected on the two hemisphere surfaces with 100 and 150 mm radii. The n sets of three linear actuators' positions and the corresponding n ball-bar lengths are measured at the

same time. In (16), δl is assumed to be zero because the ball-bar is already calibrated with respect to a length standard. Using (16) and the "lsqnonlin" function of Matlab, the kinematic parameters and the position error of the ball center are updated so as to minimize the error between the calculated and measured lengths of the ball-bar as

$$\begin{aligned} \beta' &= [\gamma_1, \gamma_2, \theta_z, \gamma_3, \theta_x, \theta_y]^T \\ &= [0.000, -0.001, 0.113, -0.006, -0.061, 0.133]^T [\text{deg}], \\ \delta q &= [-0.018, 0.017, 1.030]^T [\text{mm}]. \end{aligned}$$

From the updated kinematic parameters, it is seen that the incident angle errors between the revolute and prismatic joints are very small; however, the angle errors in the orthogonal arrangement of the three linear actuators are relatively large.

In order to demonstrate the effectiveness of the suggested calibration method, two circular tests on the

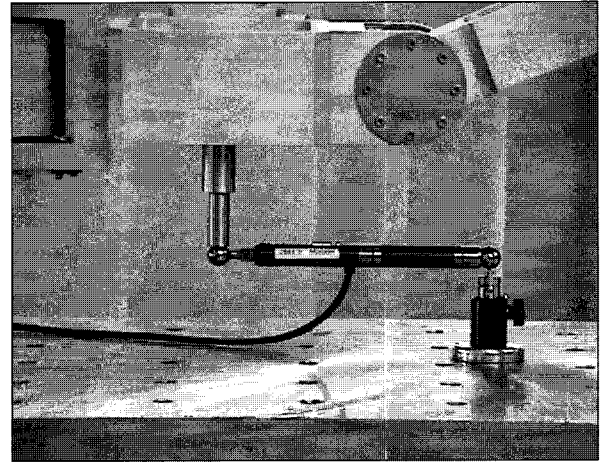


Fig. 6. Calibration experiment using a ball-bar.

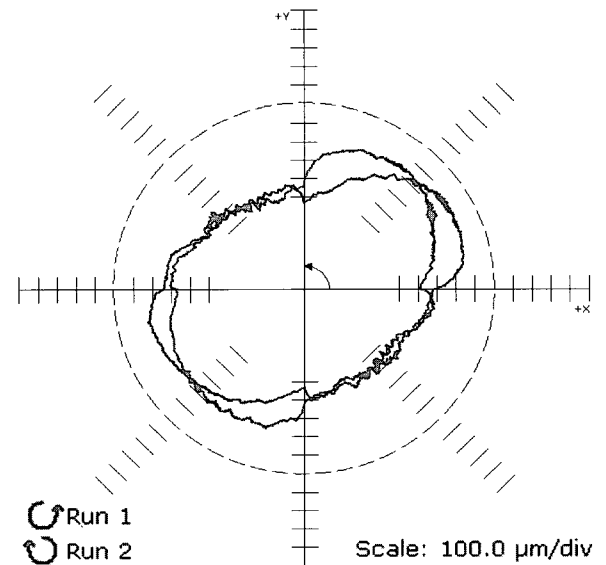


Fig. 7. Circular test before calibration.

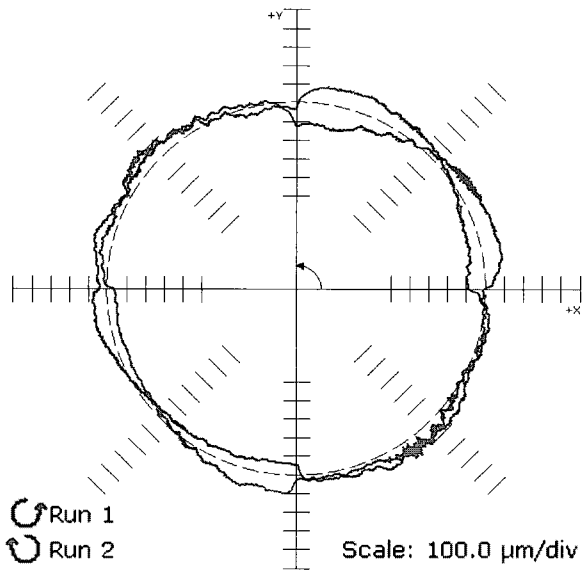


Fig. 8. Circular test after calibration.

XY plane with the radius of 150 mm are performed. Fig. 7 shows the circular test of the prototype CPM with nominal kinematic parameters. Conversely, in Fig. 8, the circular test of the machine with updated kinematic parameters is shown. In both tests, the machine was controlled to draw the circle in CCW and CW directions. From the kinematic calibration and error compensation, the maximum absolute kinematic error has been reduced from 534[μm] to 128[μm].

6. CONCLUSIONS

A prototype of a new 3-DOF translational parallel manipulator, behaving like a conventional X-Y-Z Cartesian machine, is developed. Instead of using the traditional D-H method, the geometry method is used and it is shown that based on the practical assumption, the forward kinematics for the actual model is still determined by the intersection point of the three planes. Based on the kinematic error model, two kinematic calibration methods using full position and length measurements are developed. For a full position measurement, it is derived that the calibration problem can be solved analytically. For the length measurement such as a ball-bar, a nonlinear least squares method is required. The calibration experiment on the prototype CPM using the QC10 ball-bar is performed and from the suggested calibration method, it is shown that the maximum kinematic error is reduced from 534[μm] to 128[μm].

In order to further increase the accuracy, future research will focus on the development of a general error model including a small twist angle between two

adjacent revolute joint axes and its calibration. In that case, the internal torques due to the twist angles will occur and elastic deformations due to the internal torques should be considered in the error model.

REFERENCES

- [1] K. Lee and D. K. Shah, "Kinematics analysis of a three degrees of freedom in-parallel actuated manipulator," *Proc. IEEE International Conf. on Robotics and Automation*, vol. 1, pp. 345-350, 1987.
- [2] P. H. Yang, K. J. Waldron, and D. E. Orin, "Kinematics of a three degrees-of-freedom motion platform for a low-cost driving simulator," in *Recent Advances in Robot Kinematics*, Edited by J. Lenarcic and V. Parenti-Castelli, Kluwer Academic Publishers, London, pp. 89-98, 1996.
- [3] F. Pierrot, C. Reynaud, and A. Fournier, "DELTA: A simple and efficient parallel robot," *Robotica*, vol. 8, pp. 105-109, 1990.
- [4] L. W. Tsai, G. C. Walsh, and R. Stamper, "Kinematics of a novel three DOF translational platform," *Proc. of the IEEE International Conference on Robotics and Automation*, Minneapolis, MN, pp. 3446-3451, 1996.
- [5] L. W. Tsai, "Multi-degree-of-freedom mechanisms for machine tools and the like," *U.S. Patent*, No. 5,656,905, 1997.
- [6] L. W. Tsai and S. Joshi, "Kinematics and optimization of a spatial 3-UPU parallel manipulator," *ASME Journal of Mechanical Design*, vol. 122, no. 4, pp. 439-446, 2000.
- [7] T. S. Zhao and Z. Huang, "A novel three-DOF translational platform mechanism and its kinematics," *Proc. of the ASME Design Engineering Technical Conferences*, Baltimore, MD, MECH-14101, 2000.
- [8] H. S. Kim and L. W. Tsai, "Design optimization of a cartesian parallel manipulator," *Journal of Mechanical Design*, vol. 125, no. 1, pp. 43-51, 2003.
- [9] H. S. Kim and L. W. Tsai, "Evaluation of a cartesian parallel manipulator," *Proc. of the 8th International Symposium on Advances in Robot Kinematics*, 24-28 June, Caldes de Malavella, Spain, pp. 21-28, 2002.
- [10] P. Wenger and D. Chablat, "Kinematic analysis of a new parallel machine tool: The Orthoglide," in *Advances in Robot Kinematics*, Edited by J. Lenarcic and M. L. Stanisic, Kluwer Academic Publishers, London, pp. 305-314, 2000.
- [11] J. I. Jeong, D. D. Kang, Y. M. Cho, and J. Kim, "Kinematic calibration for redundantly actuated parallel mechanisms," *Journal of Mechanical Design*, vol. 126, no. 2, pp. 307-318, 2004.
- [12] C. C. Iurascu and F. C. Park, "Geometric

- algorithms for kinematic calibration of robots containing closed loops," *Journal of Mechanical Design*, vol. 125, no. 1, pp. 23-32, 2003.
- [13] H. Ota, T. Shibukawa, and M. Uchiyama, "Forward kinematic calibration method for parallel mechanism using pose data measured by double ball bar system," *Proc. of Parallel Kinematic Machines Int. Conf.*, pp. 57-62, 2000.
- [14] A. J. Patel and K. F. Ehmann, "Calibration of a hexapod machine tool using a redundant leg," *International Journal of Machine Tools & Manufacture*, vol. 40, pp. 489-512, 2000.
- [15] Y. Takeda, G. Shen, and H. Funabashi, "A DBB-based kinematic calibration method for in-parallel actuated mechanisms using fourier series," *Journal of Mechanical Design*, vol. 126, no. 5, pp. 856-865, 2004.



Han Sung Kim received the B.S. degree in Mechanical Engineering from Hongik University, Seoul, Korea in 1994 and the M.S. and Ph.D. degrees in Mechanical Engineering from Yonsei University, Seoul, Korea in 1996 and 2000, respectively. He worked as a Postdoctoral Researcher at the University of California, Riverside,

USA from 2001 to 2003. Since 2004, he has been working in the School of Mechanical and Automation Engineering at Kyungnam University, Masan, Korea. His research interests include mechanism design, kinematics, parallel robot applications, and MEMS.